

Comparative assessment of the degradation mechanism of micro-alloyed steel in E20 and E80 simulated fuel grade ethanol environments

O. O. Joseph, C. A. Loto, S. Sivaprasad, J. A. Ajayi, and O. S. I. Fayomi

Citation: [AIP Conference Proceedings](#) **1758**, 020019 (2016); doi: 10.1063/1.4959395

View online: <http://dx.doi.org/10.1063/1.4959395>

View Table of Contents: <http://scitation.aip.org/content/aip/proceeding/aipcp/1758?ver=pdfcov>

Published by the [AIP Publishing](#)

Articles you may be interested in

[Microscopic insight into the origin of enhanced glass-forming ability of metallic melts on micro-alloying](#)
Appl. Phys. Lett. **107**, 131901 (2015); 10.1063/1.4932049

[Micro-alloying and the toughness of glasses: Modeling with pinned particles](#)
Appl. Phys. Lett. **102**, 191904 (2013); 10.1063/1.4805033

[A study of ethanol low grade as an alternative fuel for small engine](#)
AIP Conf. Proc. **1440**, 1164 (2012); 10.1063/1.4704332

[Mechanically induced structural relaxation in an amorphous metallic Fe₈₀B₂₀ alloy](#)
Appl. Phys. Lett. **68**, 319 (1996); 10.1063/1.116072

[Thermoelectric properties of mechanically alloyed p-type Si₈₀Ge₂₀ alloys](#)
AIP Conf. Proc. **217**, 431 (1991); 10.1063/1.40022

Comparative Assessment of the Degradation Mechanism of Micro-alloyed steel in E20 and E80 Simulated Fuel Grade Ethanol Environments

O.O. Joseph^{1,2*}, C.A. Loto^{1,3}, S. Sivaprasad², J.A. Ajayi⁴, O.S.I. Fayomi^{1,3}

¹*Department of Mechanical Engineering, Covenant University, P.M.B. 1023, Canaanland, Ota, Nigeria*

²*Materials Science and Technology Division, CSIR-National Metallurgical Laboratory, 831007, Jamshedpur, India*

³*Department of Chemical, Metallurgical & Materials Engineering, Tshwane University of Technology, Pretoria, South Africa*

⁴*Department of Metallurgical and Materials Engineering, Federal University of Technology, P.M.B. 704, Akure, Nigeria*

* funmi.joseph@covenantuniversity.edu.ng

Abstract. In this study, micro-alloyed steel (MAS) material normally used in the production of autoparts was immersed in gasoline (as a reference), E20 and E80 simulated fuel grade ethanol (SFGE) environment and its degradation mechanism was evaluated. Investigation of corrosion behaviour through mass loss tests and electrochemical measurements showed that no mass loss was recorded for tests in gasoline whereas lowest corrosion rate values were found in E20 and the highest values in E80. Post-corrosion SEM images of the samples after immersion tests showed degradation of MAS in E20 by crevice and pitting corrosion. On the other hand, MAS deteriorated in E80 by uniform corrosion. The presence of water and dissolved chlorides in E20 stimulated pit initiation and growth on MAS. Corrosion degradation of MAS is dependent on ethanol concentration within the tested range of 20 to 80 % ethanol.

INTRODUCTION

In order to solve the problem of global warming in the world today, biofuels are currently being used as an alternative to fossil fuels. Biofuels are biodegradable; as a result, their inadvertent spillage is of no significant environmental hazard [1,2]. Generally, biofuels such as fuel grade ethanol offers great advantages due to their chemical as well as physical characteristics, low production costs, raw materials availability and environmental friendly effects, amongst several others [3]. Furthermore, fuel grade ethanol has many favourable properties which make it preferred for fuel than its fossil counterpart. The octane number affects the anti-knocking property of the fuel while its energy yield is about one third lower than petrol [4]. Conversely, fuel grade ethanol has certain drawbacks as regards material compatibility. When ethanol is present in fuel, the fuel's chemical composition may cause corrosion on some parts of the automotive engine [5-7]. As a result, materials which normally would not corrode in gasoline may be damaged by the presence of ethanol.

In line with this, significant information has been collected from summaries, reports and reviews of studies investigating the compatibility of metallic materials with fuel grade ethanol environments [8,3,9-13]. E10 blends were found to severely corrode aluminium components, leading to catastrophic failure. With E20, dissolved chlorides and high acidity promoted pit initiation and growth in carbon steel. Of fundamental necessity is the specification of materials which syndicate corrosion resistance with high mechanical strength [14]. Micro-alloyed steels possess extensive applications, predominantly in automotive industry, gas-transmission pipelines, ship plates, bridge beams, and electrical power transmission poles, amid others [15]. They are called micro-alloyed steels because they contain only a small amount of alloying elements: vanadium, titanium or niobium. In addition, they

have a ferritic matrix with extremely fine grained structure due to the effects of the alloying elements [16]. However, there is currently sparse literature regarding the compatibility of micro-alloyed steel with fuel ethanol environments.

In view of the above, this study was undertaken to assess the corrosion behaviour of micro-alloyed steel in E20 and E80 SFGE environment. In the investigation, corrosion rates from immersion tests and anodic polarization of MAS in the fuel ethanol environments of interest were evaluated with respect to a reference test in unleaded gasoline.

EXPERIMENTAL SECTION

Materials and Test Environments

The metal samples used for this study were machined from new micro-alloyed steel plates in as-received condition. The chemical composition of this steel is shown in Table 1. Figure 1 shows the morphology of MAS in as-received condition. It consists largely of ferritic structure with lamellar pearlite randomly oriented in the ferrite matrix. The fuels used for immersion and electrochemical tests are gasoline, E20 and E80 blends which were prepared in accordance with ASTM D-4806-01a [17] for fuel grade ethanol. The reagents used for the fuel blends include: 195 proof ethanol, ultra-pure water ($\sim 18 \text{ M}\Omega/\text{cm}$), glacial acetic acid, pure methanol and pure sodium chloride (NaCl) with purity $>99\%$. In order to reach the specified NaCl and water concentrations respectively, NaCl was first dissolved in water, and then added to ethanol. The denaturant used was unleaded gasoline. The baseline composition for the SFGE used in this study is shown in Table 2. All reagents used were of analytical grade. The corrosion tests were carried out at room temperature of 27°C .

TABLE 1. Chemical composition of micro-alloyed steel in as-received condition

Element	C	Mn	Si	Cr	Ni	Al	Ti	Mo	Cu	Fe
Micro-alloyed	0.13	0.77	0.012	0.027	0.015	0.042	0.0025	0.0017	0.006	balance

TABLE 2. Composition of simulated fuel ethanol based on ASTM D4806 [17].

Ethanol (vol %)	Methanol (Vol %)	Water (vol %)	NaCl (mg/l)	Acetic Acid (mg/l)
98.5	0.5	1	32	56

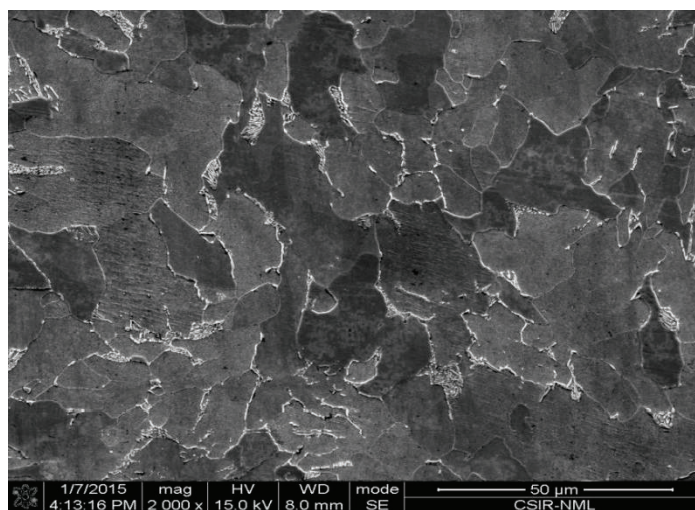


FIGURE 1. SEM images of MAS at 1000x in as-received condition.

Immersion Tests

Flat square coupons of dimensions 30 x 30 mm from 11 mm thick micro-alloyed steel plates were machined for long-term immersion tests. All specimens were dry-abraded up to 800 grit, degreased with acetone, dried and used immediately for testing. The area and weight of each specimen were measured before exposure to the test environments for the purpose of post-calculation. Duplicate samples for each test condition were suspended with nylon thread in solution for a period of 60 days. The solution was replenished every two weeks to minimize changes in solution composition as well as compensate for evaporation. After the immersion period, samples were removed, dried and cleaned in accordance with ASTM Standard G1-03 [18] for preparing, cleaning and evaluating corrosion test specimens. In addition, corrosion rate was calculated in milliliters per year using equation (1) obtained from ASTM G1-03:

$$\text{Corrosionrate} = (K \times W) / (A \times T \times D) \quad (1)$$

K is a constant (534), T is the exposure time in hours, A is the area in square inches, W is the mass loss in milligrams, D is the density in g/cm³. Sample surfaces were thereafter characterised using FEI-430 NOVA NANO FEG-SEM scanning electronmicroscope.

Electrochemical Measurements

A Gamry reference 600 Potentiostat/Galvanostat/ZRA was used for open circuit potential (OCP) and anodic polarization measurements. The test setup consists of a three electrode glass cell with saturated calomel electrode (SCE) as the reference electrode and platinum electrode as a counter electrode. Each experiment was carried out in duplicate in order to ascertain the repeatability of the experiments. All specimens were dry-abraded up to 2000 grit, degreased with acetone, dried and used immediately for testing. Samples were mounted with bakelite, thereby minimising contact area. The mounted samples were threaded to a carbon steel rod and suspended in solution. A teflon tape was used to insulate the steel rod from the test solution. The setup was designed in such a way as to maintain constant distance between the electrodes for all tests. To guarantee similar reduced metal surface, all polarization tests commenced with cathodic polarization at -0.25V vs SCE. A potential scan rate of 2 mV/s was used to reduce the effect of chloride leakage from Vycor glass as reported elsewhere [19].

RESULTS AND DISCUSSION

Corrosion Rates Determination from Immersion Tests

Figure 2 shows the corrosion rates for micro-alloyed steel after immersion in E20 and E80 fuel ethanol environments. For specimens immersed in unleaded gasoline, there was no mass loss for the test duration. A close look at the results profile reveals that there was highest corrosion rate in E80. The margin of increase in corrosion rate from 1.25E-05 mpy in E20 to 6.03E-05 mpy in E80 is quite significant, approximately 382 percent. Therefore, it can be concluded that increasing ethanol concentration up to E80 resulted in increased corrosion rate for MAS. Figure 3-4 shows the morphology of MAS after immersion in E20 and E80 for 60 days. The morphology of MAS sample immersed in E20 shows degradation by crevice and pitting corrosion whereas in E80, uniform corrosion was the prevalent failure mechanism. The occurrence of pits in MAS as a result of E20 is in agreement with the results of investigations carried out on the corrosion behaviour of carbon steel in E20 as reported literature [19]. Likely factors influencing pitting of steel in E20 are water and chloride concentrations. SFGE with less than 1 vol. % water causes no discernible pit whereas, within the range of 1-5 vol. % water content, pit size and pit density increases [19]. The influence of water on pitting of micro-alloyed steel is mainly due to weak covalent bonds formed by ethanol/water solvation [19, 20].

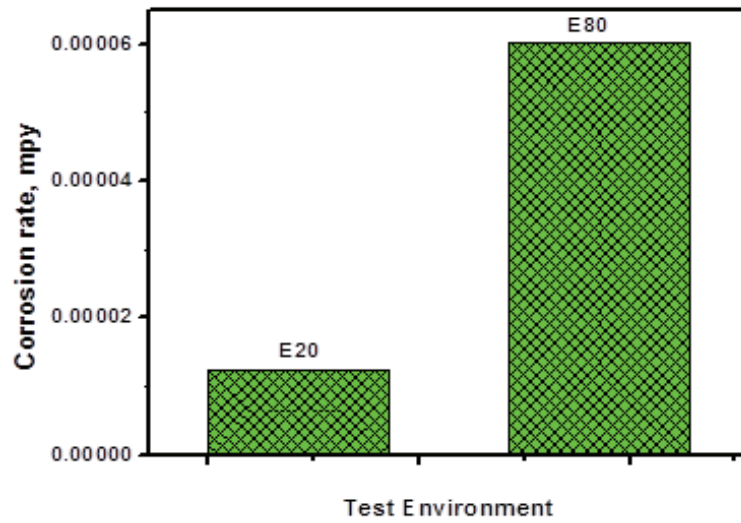


FIGURE2. Corrosion rates of MAS after immersion in E20 and E80

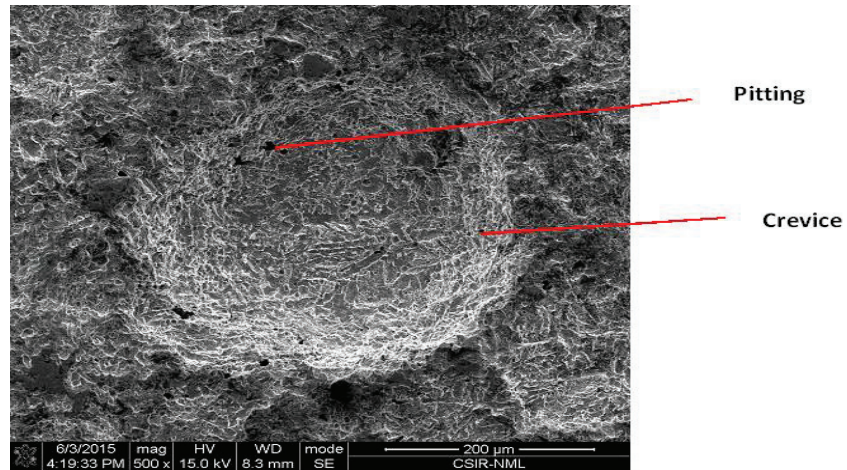


FIGURE 3. Post-corrosion SEM image of MAS at 500x after immersion in E20 for 60 days.

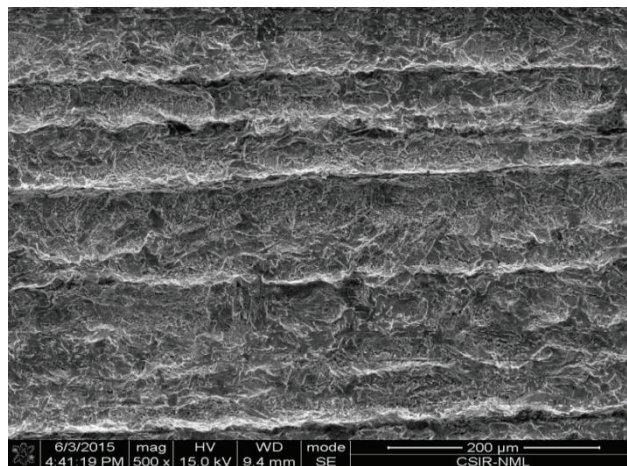


FIGURE4. Post-corrosion SEM image of MAS at 500x after immersion in E80 for 60 days.

Determination of Polarization Behaviour from Electrochemical Tests

MAS samples were anodically polarized with the same potential difference (1.5 V_{SCE}) from their initial OCPs, thereby simulating a similar effect of potential disturbance from equilibrium in the fuel ethanol environments. The result in Figure 5 shows that MAS does not exhibit clear passivation behaviour and pitting potential with anodic polarization under the range of ethanol-gasoline ratio. Calculated $i_{\text{corr-estimate}}$ from the polarization curves increased as ethanol concentration increased, which is consistent with the corrosion rate shown in Figure 2.

TABLE 3. Anodic Polarization Data for MAS in E20 and E80 environments

Test Environment	E_{corr} (mv)	$i_{\text{corr-estimate}}$ (A/cm ²)	CR (mpy)
E20 + 32 mg/l NaCl	-4.40E+02	2.41E-06	1.07E+00
E80 + 32 mg/l NaCl	-4.13E+02	8.27E-05	3.69E+01

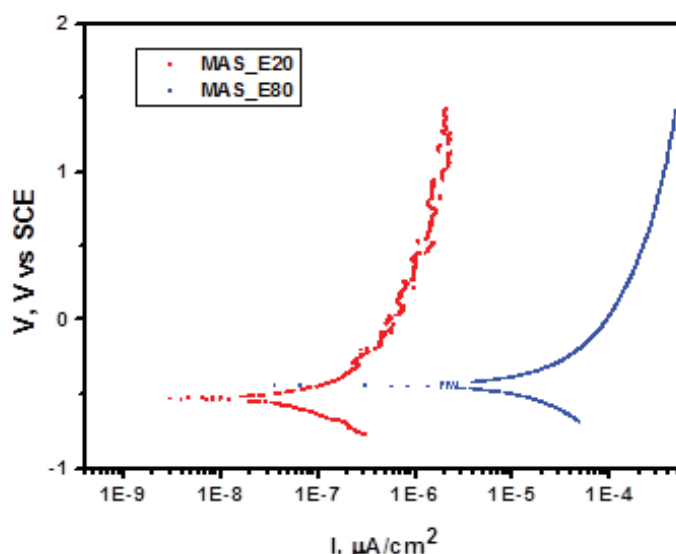


FIGURE 5. Typical anodic polarization curves for MAS in E20 and E80 simulated fuel grade ethanol.

CONCLUSIONS

The degradation mechanism of micro-alloyed steel in simulated fuel grade ethanol has been systematically studied with variations in ethanol concentration. The electrochemical properties of MAS surface were found to be sensitive to the contaminants in SFGE. The specific conclusions arrived at are as follows:

- Corrosion rate increased with increasing ethanol concentration. In unleaded gasoline, there was no mass loss; as a result, corrosion rate was zero.
- Electrochemical measurements exhibited no clear passivation and pitting potential of MAS. The $i_{\text{corr-estimate}}$ measured from the polarization curves, increased due to increasing ethanol concentration, which presents a comparable trend to the mass loss results.
- MAS sample immersed in E20 shows degradation by crevice and pitting corrosion whereas in E80, uniform corrosion was the prevalent failure mechanism.

ACKNOWLEDGEMENTS

This work was sponsored by CSIR-National Metallurgical Laboratory, Jamshedpur, India and The World Academy of Sciences (TWAS), Trieste, Italy in collaboration with Covenant University, Ota, Nigeria under the CSIR-TWAS Postgraduate fellowship scheme (FR No. 3240275047).

REFERENCES

1. B. K. Highina, I. M. Bugaje and B. Umar, *J. Pet. Tech. Dev.* **1**, 1-15 (2012).
2. M. Munoz, F. Moreno and J. Morea, *Trans ASAE (Am. Soc. Agric. Eng.)* **47**, 5-11 (2004).
3. L. M. Baena, M. Gomez and J. A. Calderon, *Fuel* **95**, 320-328 (2012).
4. V. Micic and M. Jotanovic, *Zastita Materijala* **56**, 403-408 (2015).
5. R. D. Kane, J. G. Maldonado and L. J. Klein, Stress corrosion cracking in fuel ethanol: a newly recognized phenomenon in Corrosion 2004, NACE conference and Proceedings (NACE International, San Antonio, Texas, 2004), pp. 1-16.
6. R. D. Kane, N. Sridhar, M. Brongers, J. A. Beavers, A. K. Agarwal and L. Klein, *Mater. Performance* **44**, 50-55 (2005).
7. J. P. De Souza, O. R. Mattos, L. Sathler and H. Takenouti, *Corros. Sci.* **27**, 1351-1364.
8. Minnesota Pollution Control Agency, *E20: the feasibility of 20 percent ethanol blends by volume as a motor fuel, executive summary results of materials compatibility and drivability testing* (Minnesota Department of Agriculture, USA, 2008), pp. 1-6.
9. L. R. Goodman and P. M. Singh, *Corros. Sci.* **65**, 238-248 (2012).
10. S. Wall, *Assessing compatibility of fuel systems with bio-ethanol and the risk of carburettor icing* (Qinetiq, Farnborough, 2010), pp. 1-54.
11. X. Lou, D. Yang, R. L. Goodman and P. M. Singh, "Understanding the stress corrosion cracking of X-65 pipeline steel in fuel grade ethanol" in *Corrosion 2010*, NACE conference and Proceedings (NACE International, San Antonio, Texas, 2010), pp. 1-10.
12. Concawe Special Task Force, FE/STF-24, *Guidelines for handling and blending motor gasoline containing up to 10% v/v ethanol* (Concawe, Brussels, 2008), pp. 1-18.
13. J. A. Beavers, M. P. Brongers, A. K. Agarwal and F. A. Tallarida, "Prevention of internal SCC in ethanol pipelines" in *Corrosion 2008*, NACE conference and Proceedings (NACE International, New Orleans, Louisiana, 2008), pp. 1-24.
14. Y. Prawoto, K. Ibrahim and W. B. Wan Nik, *Arab J. Sci. Eng.* **34**, 115-127 (2009).
15. M. A. Lucio-Garcia, J. G. Gonzalez-Rodriguez, M. Casales, L. Martinez, J. G. Chacon-Nava, M. A. Neri-Flores and A. Martinez-Villafane, *Corros. Sci.* **51**, 2380-2386 (2009).
16. E. M. Sherif and A. H. Seikh, *Int. J. Electrochem. Sci.* **7**, 7567-7578 (2012).
17. ASTM-D-4806-01a, *Standard Specification for Denatured Fuel ethanol for Blending with Gasolines for Use as Automotive Spark-Ignition Engine Fuel* (ASTM International, West Conshohocken, PA, USA, 2001), pp. 1-8.
18. ASTM G1-03, *Standard Practice for Preparing, Cleaning and Evaluating Corrosion Test Specimens* (ASTM International, West Conshohocken, PA, USA, 2011), pp. 1-9.
19. X. Lou and P. M. Singh, *Corros. Sci.* **52**, 2303-2315 (2010).
20. S. A. Shchukarev and T. A. Tolmacheva, *J. Struct. Chem.* **9**, 6-21 (1968).